The Astrophysical Journal Letters, 723:L122–L126, 2010 November 1 doi:10.1088/2041-8205/723/1/L122

GAMMA-RAY EMISSION FROM CRUSHED CLOUDS IN SUPERNOVA REMNANTS

Yasunobu Uchiyama[1], Roger D. Blandford[1], Stefan Funk[1], Hiroyasu Tajima[2], and Takaaki Tanaka[3]
[1] SLAC National Accelerator Laboratory, 2575 Sand Hill Road M/S 29, Menlo Park, CA 94025, USA; uchiyama@slac.stanford.edu
[2] Solar-Terrestrial Environment Laboratory, Nagoya University, Furo-cho, Chikusa-ku, Nagoya 464-8601, Japan
[3] Kavli Institute for Particle Astrophysics and Cosmology, Stanford University, 382 Via Pueblo Mall, MC 4060, Stanford, CA 94305-4060, USA
Received 2010 August 10; accepted 2010 September 29; published 2010 October 14

ABSTRACT

It is shown that the radio and gamma-ray emission observed from newly found "GeV-bright" supernova remnants (SNRs) can be explained by a model in which a shocked cloud and shock-accelerated cosmic rays (CRs) frozen in it are simultaneously compressed by the supernova blast wave as a result of formation of a radiative cloud shock. Simple reacceleration of pre-existing CRs is generally sufficient to power the observed gamma-ray emission through the decays of π^0-mesons produced in hadronic interactions between high-energy protons (nuclei) and gas in the compressed-cloud layer. This model provides a natural account of the observed synchrotron radiation in SNRs W51C, W44, and IC 443 with flat radio spectral index, which can be ascribed to a combination of secondary and reaccelerated electrons and positrons.

Key words: acceleration of particles – cosmic rays – radiation mechanisms: non-thermal

Online-only material: color figures

1. INTRODUCTION

Luminous extended GeV γ-ray emission associated with middle-aged supernova remnants (SNRs) has recently been unveiled by the Large Area Telescope (LAT) on board the *Fermi Gamma-ray Space Telescope*. Specifically, SNRs W51C, W44, IC 443, and W28 are spatially resolved with the *Fermi* LAT (Abdo et al. 2009, 2010a, 2010b, 2010c). The four SNRs are interacting with molecular clouds, as evidenced, e.g., by 1720 MHz OH maser emission. The radio and γ-ray emission from these SNRs share similar characteristics. The synchrotron radio emission has a large flux of 160–310 Jy at 1 GHz with flat spectral index of $\alpha \simeq 0.26$–0.40. The GeV γ-ray spectrum commonly exhibits a spectral break at around 1–10 GeV, and the luminosity ranges $L_\gamma = (0.8\text{–}9) \times 10^{35}$ erg s^{-1} in the 1–100 GeV band. Other cloud-interacting SNRs associated with the LAT sources, such as CTB 37A, also emit γ-rays at a luminosity of $L_\gamma \sim 10^{35}$ erg s^{-1} (Castro & Slane 2010).

A prototypical example of the GeV-bright SNRs is SNR W44. The radio continuum map of W44 exhibits filamentary and sheet-like structures of synchrotron radiation well correlated with the shocked H_2 emission (Reach et al. 2005; Castelletti et al. 2007). According to Reach et al. (2005), the bulk of the synchrotron radiation can be ascribed to a fast molecular shock of a velocity $v_s \sim 100$ km s^{-1} advancing through a molecular cloud of a preshock density $n_0 \sim 200$ cm^{-3}. By passage of the blast wave of the SNR, the shocked molecular cloud forms a thin sheet due to radiative cooling. The radio filaments are thought to come from the compressed zone behind the shock front.

The synchrotron radio emission arising from such a "crushed cloud" was modeled by Blandford & Cowie (1982). It was shown that reacceleration of pre-existing cosmic ray (CR) electrons at a cloud shock and subsequent adiabatic compression results in enhanced synchrotron radiation, capable of explaining the radio intensity from evolved SNRs. Bykov et al. (2000) discussed a similar scenario in which direct electron acceleration from the thermal pool is also invoked.

The π^0-decay γ-ray emission should be enhanced in the crushed clouds in the same manner as the synchrotron radiation. In this Letter, we demonstrate that the newly found γ-ray emission from middle-aged SNRs can be readily understood within the crushed cloud scenario in which the γ-ray emission comes from shocked clouds overrun by SNR blast waves. It should be emphasized that our model is essentially different from the scenarios adopted in the recent papers (e.g., Fujita et al. 2010; Torres et al. 2010), where molecular clouds in the vicinity of SNRs are assumed to be illuminated by runaway CRs (Aharonian & Atoyan 1996; Gabici et al. 2009). While the GeV and TeV γ-rays outside the southern boundary of SNR W28 (Aharonian et al. 2008; Giuliani et al. 2010; Abdo et al. 2010c) may be explained by such runaway CRs, we argue here that the luminous GeV γ-ray emission in the directions of cloud-interacting SNRs emerges from the radiatively compressed clouds.

2. THE MODEL

2.1. Cloud Shock Structure

Let us consider a strong shock driven into a molecular cloud by the high pressure behind a supernova blast wave. Using the number density of hydrogen nucleus in the preshock cloud, n_0, the preshock magnetic field is described by a dimensionless parameter b:

$$B_0 = b\sqrt{(n_0/\mathrm{cm}^{-3})}\ \mu\mathrm{G}. \quad (1)$$

Zeeman measurements of self-gravitating molecular clouds show that b is roughly constant from one cloud to another with $b \sim 1$ (Crutcher 1999). We are concerned primarily with a fast ($v_s \gtrsim 50$ km s^{-1}) J-type shock (Draine 1980) in which ambipolar diffusion and radiative cooling are unimportant in a shock dissipation layer. The steady-state postshock structure of a fast molecular shock is described in Hollenbach & McKee (1989), which is referred to as HM89 hereafter.

The initial temperature immediately behind the shock front is $T_s \simeq 3.2 \times 10^5\, v_{s7}^2/x_t$ K, where $v_{s7} \equiv v_s/(100$ km s$^{-1})$, and x_t is the number of particles per hydrogen nucleus (HM89). The density rises from a preshock density n_0 by a factor of $r_{sh} = 4$, in the strong shock limit. For $v_{s7} \gtrsim 1.2$, ionizing radiation produced in the immediate postshock layer is strong enough to fully predissociate and preionize the upstream cloud.

As the gas radiatively cools downstream, the temperature decreases and the density increases. The compression of the cooling gas is limited by the magnetic pressure in the cases that we shall be considering. The density of the cooled gas, n_m, is determined as

$$n_m \simeq 94\, n_0 v_{s7} b^{-1}, \quad (2)$$

which is obtained by equating $B_m^2/8\pi$ with the shock ram pressure $n_0 \mu_{\rm H} v_s^2$, where $B_m = \sqrt{2/3}(n_m/n_0)B_0$ is the compressed magnetic field and $\mu_{\rm H}$ is the mass per hydrogen nucleus (HM89). (We have assumed that the preshock magnetic field is randomly directed.) The [O I] line (63μm) surface brightness of a face-on J-shock is proportional to the particle flux into the shock, $n_0 v_s$. The peak surface brightness of the [O I] line is 1×10^{-3} erg cm^{-2} s^{-1} sr^{-1} in SNR W44 (Reach & Rho 1996), and a factor of two smaller in IC 443 (Rho et al. 2001), indicating the particle flux of order $n_0 v_s \sim 10^9$ cm^{-2} s^{-1} (HM89) and therefore $n_m \sim 9 \times 10^3\, b^{-1}$ cm^{-3}.

A certain column density, $N_{\rm cool}$, has to be transmitted by a shock for gas to cool down to 10^4 K and become radiative. This occurs in a column density $N_{\rm cool} \simeq 3 \times 10^{17}\, v_{s7}^4$ cm^{-2} for $v_{s7} = 0.6$–1.5 (McKee et al. 1987). Recombination and photoionization by the ultraviolet radiation produced upstream are balanced in $N_{\rm cool} < N < N_{\rm ion} \sim 10^{19}$ cm^{-2}. Beyond $N_{\rm ion}$, the ionizing photons are absorbed and molecular chemistry commences. By setting a typical elapsed time since shocked to be $t_c = t/2$, where $t = 10^4\, t_4$ yr is the age of the remnant, and using $n_{0,2} \equiv n_0/(100$ cm$^{-2})$, the column density of the compressed cloud is written as $N_c = n_0 v_s t_c \simeq 1.5 \times 10^{20} n_{0,2} v_{s7} t_4$ cm^{-2}.

The bulk of synchrotron radio waves and γ-rays should be emitted in the compressed gas with a constant density n_m (within a factor of two) and magnetic field B_m. Note that we idealize the shock as one dimensional and ignore any effects, such as lateral compression, caused by the secondary shocks. The secondary shocks could affect the leakage of high-energy particles from the compressed cloud, playing an indirect role in the γ-ray production. Also, the ultraviolet radiation produced in the secondary shocks may change the ionization level of the precursor of the main cloud shock.

2.2. Shock Acceleration and Adiabatic Compression

Following Blandford & Cowie (1982), we consider a conservative case in which only pre-existing CRs are accelerated by the process of diffusive shock acceleration at a cloud shock. Suprathermal particles may be injected to the acceleration process at the shock front, despite slow acceleration and fast Coulomb losses. However, we shall show below that the shock acceleration of pre-existing CRs alone appears to suffice as the origin of the observed γ-ray emission from the cloud-interacting SNRs, and therefore consider the reacceleration case only.

Let $n_{\rm acc}(p)dp$ be the CR number density in $p \sim p + dp$, transmitted by a shock, and $n_{\rm GCR}(p)$ be the pre-existing ambient CR density. According to the theory of diffusive shock acceleration (Blandford & Eichler 1987), for $p < p_{\rm br/max}$ (see below),

$$n_{\rm acc}(p) = (\alpha + 2)\, p^{-\alpha} \int_0^p dp' n_{\rm GCR}(p')\, p'^{(\alpha-1)}, \quad (3)$$

where $\alpha = (r_{\rm sh} + 2)/(r_{\rm sh} - 1)$ and $r_{\rm sh}$ is the shock compression ratio, which is assumed to be $r_{\rm sh} = 4$.

Assuming that the density of the Galactic CRs in the molecular cloud is same as that in the general interstellar medium, we adopt the Galactic CR proton spectrum of the form

$$n_{\rm GCR,p}(p) = 4\pi J_p \beta^{1.5} p_0^{-2.76}, \quad (4)$$

where $p_0 = p/({\rm GeV}/c)$, $J_p = 1.9$ cm^{-2} s^{-1} sr^{-1} GeV^{-1}, β is the proton velocity in units of c. A low-energy cutoff at a kinetic energy of 50 MeV is applied. This spectrum lies in between Shikaze et al. (2007) and Strong et al. (2004) at 100 MeV. For the CR electron+positron spectrum, we use

$$n_{\rm GCR,e}(p) = 4\pi J_e p_0^{-2} \left(1 + p_0^2\right)^{-0.55}, \quad (5)$$

extending down to a low-energy cutoff of 20 MeV at which point ionization losses in the Galaxy should make the spectrum flat. The normalization factor is $J_e = 2 \times 10^{-2}$ cm^{-2} s^{-1} sr^{-1} GeV^{-1}.

The preshock upstream gas is only partially ionized for $v_{s7} \lesssim 1.2$. Recently, Malkov et al. (2010) have proposed that strong ion–neutral collisions accompanying Alfvén wave evanescence lead to steepening of the spectrum of accelerated particles; the slope of the particle momentum distribution becomes steeper by one power above $p_{\rm br} = 2eB_0 V_{\rm A}/c\nu_{\rm i-n}$, where V_A is the Alfvén velocity and $\nu_{\rm i-n} \simeq 9 \times 10^{-9}\, n_{\rm n,0} T_4^{0.4}$ s^{-1} is the ion–neutral collision frequency. Here, $n_{\rm n,0}$ denotes the density of neutrals in units of cm^{-3} and T_4 is the precursor temperature in units of 10^4 K. Interestingly, the parameters of Reach et al. (2005) estimated for the radio filaments of W44, namely, $v_{s7} \sim 1$ and $n_{0,2} \sim 2$, together with $B_0 = 30\,\mu$G and $T_4 = 1$ predict $p_{\rm br} \sim 10$ GeV/c using the precursor ionization fraction calculated by HM89. This agrees with the break value measured by the *Fermi* LAT (Abdo et al. 2010a). We introduce spectral steepening to $n_{\rm acc}(p)$, by multiplying a factor of $p_{\rm br}/p$ above $p_{\rm br}$.

Even if the preshock gas is fully ionized, spectral steepening due to a finite acceleration time would be unavoidable already in the *Fermi* bandpass. The timescale of diffusive shock acceleration can be written as $t_{\rm acc} \simeq (10/3)\eta c r_g v_s^{-2}$, where $r_g = cp/eB_0$ is the gyroradius and $\eta \geqslant 1$ is the gyrofactor; $\eta \sim 1$ has been obtained in young SNRs like RX J1713.7−3946 (Uchiyama et al. 2007). Equating $t_{\rm acc}$ with t_c, the maximum attainable energy is obtained as $cp_{\rm max} \simeq 50\,(\eta/10)^{-1} v_{s7}^2 B_{-5} t_4$ GeV, where $B_{-5} = B_0/(10^{-5}$ G). A factor of $\exp[-(p/p_{\rm max})]$ is multiplied with $n_{\rm acc}(p)$ to introduce the maximum attainable energy.

The high-energy particles accelerated at the shock experience further heating due to adiabatic compression, as the gas density increases until the pressure is magnetically supported. Each particle gains energy as $p \rightarrow s^{1/3} p$, where $s \equiv (n_m/n_0)/r_{\rm sh}$, and the density increases by a factor of s (see Blandford & Cowie 1982). Therefore, the number density of accelerated and compressed CRs at the point where the density becomes $\sim n_m$ is

$$n_{\rm ad}(p) = s^{2/3} n_{\rm acc}(s^{-1/3} p). \quad (6)$$

2.3. Evolution in the Compressed Region

In the compressed region of the cloud with a constant density $\sim n_m$, high-energy particles suffer from energy losses such as Coulomb/ionization losses. Also, the production of secondaries in inelastic proton–proton collisions can be a significant source of high-energy electrons and positrons, since the energy loss timescale due to the pp collisions, $t_{pp} \simeq 6 \times 10^7\, (n_m/{\rm cm}^{-3})^{-1}$ yr, generally becomes comparable to t_c.

Let $N_p(p, t)dp$ represent the number of protons in $p \sim p+dp$ integrated over the emission volume at time t. We employ a usual

Table 1
Model Parameters for SNR W44

Parameters	Values
Assumed SNR dynamics	
Distance: D	2.9 kpc[a]
Radius: R	12.5 pc[a]
	($\theta = 15'$)
Age: t	10000 yr[a]
Explosion energy: E_{51}	5[a]
Preshock cloud parameters	
Density: n_0	200 cm^{-3}[a]
Filling factor: f	0.18
Magnetic field: B_0	25 μG
Dependent parameters	
Cloud shock velocity: v_s	100 km s^{-1}[a]
Break momentum ($T_4 = 2$): $p_{\rm br}$	7 GeV/c
Maximum momentum ($\eta = 10$): $p_{\rm max}$	122 GeV/c

Note. [a] Taken from Reach et al. (2005).

kinetic equation to obtain the proton spectrum $N_p(p, t)$:

$$\frac{\partial N_p(p,t)}{\partial t} = \frac{\partial}{\partial p}[b(p)N_p(p,t)] + Q_p(p), \quad (7)$$

where Q_p is the proton injection rate and $b(p) = -\dot{p}$ represents the proton energy losses. Charged particles with $p < p_{\rm max}$ are assumed to be effectively trapped within the compressed gas. The particle spectrum for accelerated electrons, $N_e(p, t)$, and for secondary $e^{\pm}$ resulting from hadronic interactions, $N_{\rm sec}(p, t)$, are computed similarly.

The injection rates of primaries are related to $n_{\rm ad}(p)$:

$$Q(p) = \frac{n_0 f V}{n_m t_c} n_{\rm ad}(p), \quad (8)$$

where $V = 4\pi R^3/3$ is the SNR volume with a radius R and f is the preshock filling factor of the compressed cloud. The volume of the preshock cloud is then fV. For simplicity, we assume that $Q(p)$ for primaries is time independent; v_s is assumed to be constant and $p_{\rm max}$ is evaluated simply at $t = t_c$. The injection rate of secondary $e^{\pm}$, $Q_{\rm sec}(p_e, t)$, is determined by $N_p(p_p, t)$ following the prescription given by Kamae et al. (2006).

2.4. SNR Dynamics

It may be desirable to relate the cloud shock velocity with the physical parameters that describe the blast wave of the remnant. We consider a remnant in the Sedov stage[4]:

$$R_{12.5} = \left(\frac{E_{51}}{n_{\rm a,0}}\right)^{1/5} t_4^{2/5}, \quad (9)$$

where $R_{12.5} = R/(12.5\ {\rm pc})$, E_{51} denotes the kinetic energy released by the supernova in units of 10^{51} erg and $n_{\rm a,0} = n_{\rm a}/({\rm cm}^{-3})$ represents the ambient (intercloud) density. The blast wave velocity is $v_{\rm b} = 0.4R/t$. When a molecular cloud is struck by the blast wave, a strong shock is driven into the cloud with a shock velocity of

$$v_{\rm s} = k\left(\frac{n_{\rm a}}{n_0}\right)^{1/2} v_{\rm b}, \simeq 65\, n_{0,2}^{-1/2} E_{51}^{1/2} R_{12.5}^{-3/2}\ {\rm km\ s^{-1}}, \quad (10)$$

[4] This implies $t < t_{\rm tr}$, where $t_{\rm tr}$ is an age for transition to the radiative phase of SNR evolution (Blondin et al. 1998): $t_{\rm tr} \sim 3 \times 10^4\ E_{51}^{4/17}\ n_{\rm a,0}^{-9/17}$ yr.

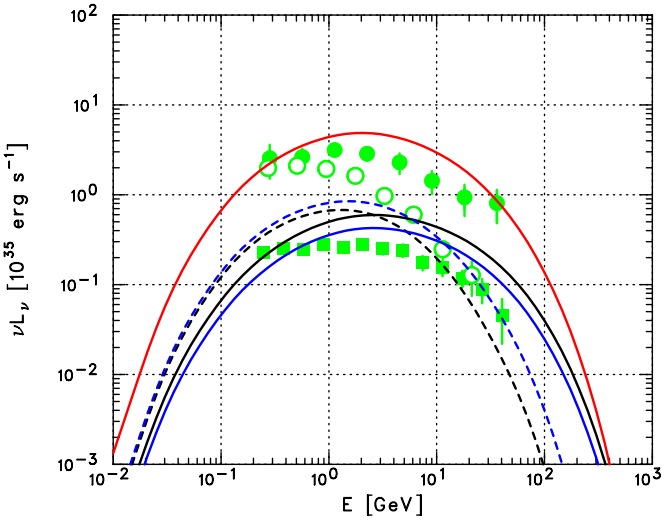

Figure 1. π^0-decay γ-ray spectra calculated for the reacceleration model using various sets of parameters. Spectral data points are for SNR W51C (filled circles: Abdo et al. 2009), W44 (open circles: Abdo et al. 2010a), and IC 443 (squares: Abdo et al. 2010b).

(A color version of this figure is available in the online journal.)

where $k \simeq 1.3$ is adopted. Note that k depends weakly on $v_{\rm s}/v_{\rm b}$ (McKee & Cowie 1975), ranging $k = 1$–1.5 in the circumstances of our interest. To drive a fast molecular shock of $v_{s7} \gtrsim 0.5$ into a molecular cloud, a condition of

$$n_{0,2} \lesssim k^2\, E_{51}\, R_{12.5}^{-3} \quad (11)$$

must be satisfied.

3. RESULTS

Let us calculate the nonthermal radiation arising from the radiatively compressed clouds. The gas density and magnetic field strength are constant over the emission volume in which high-energy particles are distributed with the volume-integrated spectrum of $N(p, t_c)$. Leptonic components include synchrotron radiation, inverse-Compton scattering, and relativistic bremsstrahlung; the inverse-Compton emission is negligible as compared to the bremsstrahlung component (see, e.g., Abdo et al. 2010a). Inelastic collisions between CR protons/nuclei and gas nuclei lead to π^0-decay γ-ray emission, which constitutes the main component in the *Fermi*-LAT band under the assumption that only pre-existing CRs can be accelerated at the cloud shock.

We do not consider the densest part of the interacting molecular cloud. For example, detections of OH(1720 MHz) maser emission (Frail et al. 1996) indicate the presence of slow C-type shocks in dense molecular clumps, say $v_{s7} \sim 0.3$ and $n_{0,2} \sim 10$, in addition to the fast J-type shock described in Section 2. However, the γ-ray emission from the slow non-dissociative shocks is not expected to be strong because of inefficient shock acceleration and weaker gas compression (see also Bykov et al. 2000). Indeed, the contribution from such dense molecular clumps to the total radio intensity appears small in SNR W44 (Reach et al. 2005). The largest preshock density we should consider is given by Equation (11). Also, we ignore the blast wave region, since the radiative compression is essential in our model.

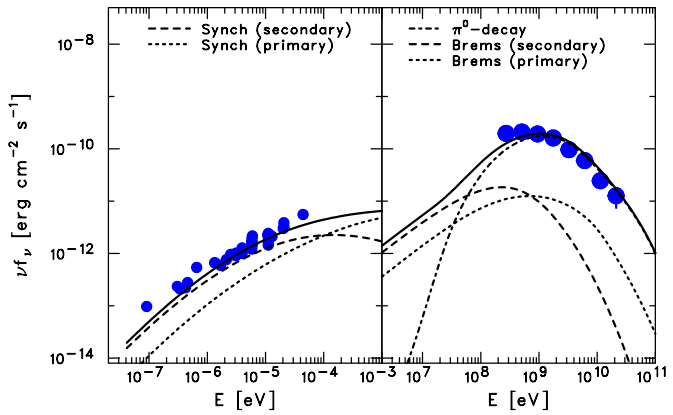

Figure 2. Radio (left) and γ-ray (right) spectra of SNR W44 together with the reacceleration model using the parameters in Table 1, most of which are copied from Reach et al. (2005). The radio fluxes are scaled by a factor of 0.5 (see the text).

(A color version of this figure is available in the online journal.)

3.1. Gamma-ray Luminosity

We show here that the γ-ray luminosity anticipated within this scenario agrees well with the observed luminosity of $\sim 10^{35}$ erg s^{-1}. In Figure 1, the γ-ray spectra of SNRs W51C, W44, and IC 443 measured with the *Fermi* LAT are shown in the so-called νL_ν form in units of 10^{35} erg s^{-1}. The LAT spectral points are taken from Abdo et al. (2009, 2010a, 2010b) and converted into the νL_ν form using the distances of 6 kpc (W51C), 2.9 kpc (W44), and 1.5 kpc (IC 443).

To demonstrate the expected level of the γ-ray luminosity, we present the spectra of π^0-decay γ-rays with varying R, n_0, and E_{51}. The following parameters are fixed: $b = 2$, $f = 0.2$, $n_{a,0} = 1$. Also, $p_{\rm max}$ is set by adopting $\eta = 10$, and $p_{\rm br}$ is set by $T_4 = 2$ and by the ionization fraction calculated based on HM89, here and hereafter. The γ-ray spectra simply scale as $\propto f$, and depend very weakly on n_a. The black lines in Figure 1 show the results obtained for $n_{0,2} = 0.3$ (solid curve) and $n_{0,2} = 3$ (dashed curve) in the case of $R = 10$ pc and $E_{51} = 1$. The γ-ray luminosity around 1 GeV varies only within a factor of ~ 2 between $n_{0,2} = 0.3$ and $n_{0,2} = 3$, while that at 100 GeV changes more than an order of magnitude. On the other hand, the blue lines in Figure 1 show the spectra calculated for $R = 5$ pc (solid curve) and $R = 15$ pc (dashed curve) in the case of $n_{0,2} = 1$ and $E_{51} = 1$. The γ-ray luminosity differs by a factor of ~ 3. We note that the shocked cloud mass amounts to $\sim 10^4\,M_\odot$ in the case of $R = 15$ pc. Finally, to explore the most luminous scenario, we adopt $E_{51} = 5$ together with $R = 30$ pc and $n_{0,2} = 1$ (red curve). The γ-ray luminosity reaches $\sim 10^{36}$ erg s^{-1}, in good agreement with the observations of SNR W51C, which is indeed the most luminous SNRs in gamma-rays. Our model generally predicts $L_\gamma \sim 10^{35}\,(f/0.2)\,E_{51}^{2/3}$ erg s^{-1} to the first order, which led us to conclude that the *Fermi*-detected γ-rays are quite likely due to the decays of π^0-mesons produced by the pre-existing CRs accelerated and subsequently compressed in the shocked cloud.

3.2. Flat Radio Spectra

The GeV-bright SNRs W51C, W44, and IC 443 are also radio-bright objects. As shell-type SNRs, their radio spectra are remarkably flat with a spectral index of $\alpha \simeq 0.26$ (W51C: Moon & Koo 1994), $\alpha \simeq 0.37$ (W44: Castelletti et al. 2007), and $\alpha \simeq 0.36$ (IC 443: Erickson & Mahoney 1985), with a typical uncertainty of 0.02, being inconsistent with $\alpha = 0.5$ that is expected by shock-acceleration theory. Our model naturally explains the flat radio spectrum. Let us demonstrate by presenting the radio and γ-ray modeling of SNR W44 how the radio and γ-ray spectra can be simultaneously reproduced.

Radio (Castelletti et al. 2007) and γ-ray (Abdo et al. 2010a) spectra of SNR W44 are shown in Figure 2. One half of the total synchrotron flux measured for W44 is assumed to originate in a fast molecular shock, which is roughly consistent with Table 2 of Reach et al. (2005). The rest is attributed to the blast wave region. Table 2 of Reach et al. (2005) was chosen as an initial set of model parameters: $R_{12.5} = 1$, $t_4 = 1$, $E_{51} = 5$, and $n_{0,2} = 2$. We then attempted to reproduce the nonthermal radiation spectra by varying f and B_0, and found that $f = 0.18$ and $B_0 = 25\,\mu$G provide a good fit to the data (see Table 1 and Figure 2). The radio measurements can be reconciled with this model in which the synchrotron radiation is largely contributed by secondary electrons and positrons. The flat radio spectrum is generically expected in our model.

4. DISCUSSION

The radiatively compressed cloud provides a simple explanation for the radio and γ-ray data. Interestingly, the observed steepening in the γ-ray spectra is successfully reproduced by $p_{\rm br}$ in the case of SNR W44. However, there may be other explanations for the steepening. For example, high-energy particles may be prone to escape from the compressed magnetized cloud. Also, the spectral break may be due to the fact that the crushed clouds have a range of n_0. A superposition of γ-ray spectra characterized by different $p_{\rm max}$ (as a result of different n_0) could look like a break. We are primarily interested in understanding the γ-ray luminosity rather than the spectral shape in this Letter, and therefore we did not explore this issue.

The simple reacceleration of pre-existing CRs and subsequent compression alone would not fully explain the γ-rays associated with cloud-interacting SNRs. For example, the GeV–TeV γ-ray emission found outside the radio boundary of SNR W28 (Aharonian et al. 2008; Giuliani et al. 2010; Abdo et al. 2010c) may represent the molecular cloud illuminated by runaway CRs (Aharonian & Atoyan 1996; Gabici et al. 2009). Also, we assumed pre-existing CRs in the cloud to have the same spectra as the galactic CRs in the vicinity of the solar system. However, the ambient CRs in the pre-shock cloud may deviate from the galactic pool due to the runaway CRs that have escaped from SNR shocks at earlier epochs. If this is the case, modeling of the γ-ray spectrum, at TeV energies in particular, should take into account modified pre-existing CRs in the pre-shock cloud.

We acknowledge the useful suggestions of the anonymous referee, which improved the manuscript. We thank Heinz Völk and Felix Aharonian for valuable discussions.

REFERENCES

Abdo, A. A., et al. 2009, ApJ, 706, L1
Abdo, A. A., et al. 2010a, Science, 327, 1103
Abdo, A. A., et al. 2010b, ApJ, 712, 459
Abdo, A. A., et al. 2010c, ApJ, 718, 348
Aharonian, F. A., & Atoyan, A. M. 1996, A&A, 309, 917
Aharonian, F., et al. 2008, A&A, 481, 401
Blandford, R. D., & Cowie, L. L. 1982, ApJ, 260, 625
Blandford, R., & Eichler, D. 1987, Phys. Rep., 154, 1
Blondin, J. M., Wright, E. B., Borkowski, K. J., & Reynolds, S. P. 1998, ApJ, 500, 342

Bykov, A. M., Chevalier, R. A., Ellison, D. C., & Uvarov, Y. A. 2000, ApJ, 538, 203
Castelletti, G., Dubner, G., Brogan, C., & Kassim, N. E. 2007, A&A, 471, 537
Castro, D., & Slane, P. 2010, ApJ, 717, 372
Crutcher, R. M. 1999, ApJ, 520, 706
Draine, B. T. 1980, ApJ, 241, 1021
Erickson, W. C., & Mahoney, M. J. 1985, ApJ, 290, 596
Frail, D. A., Goss, W. M., Reynoso, E. M., Giacani, E. B., Green, A. J., & Otrupcek, R. 1996, AJ, 111, 1651
Fujita, Y., Ohira, Y., & Takahara, F. 2010, ApJ, 712, L153
Gabici, S., Aharonian, F. A., & Casanova, S. 2009, MNRAS, 396, 1629
Giuliani, A., et al. 2010, A&A, 516, L11
Hollenbach, D., & McKee, C. F. 1989, ApJ, 342, 306 (HM89)
Kamae, T., Karlsson, N., Mizuno, T., Abe, T., & Koi, T. 2006, ApJ, 647, 692
Malkov, M. A., Diamond, P. H., & Sagdeev, R. Z. 2010, arXiv:1004.4714
McKee, C. F., & Cowie, L. L. 1975, ApJ, 195, 715
McKee, C. F., Hollenbach, D. J., Seab, G. C., & Tielens, A. G. G. M. 1987, ApJ, 318, 674
Moon, D.-S., & Koo, B.-C. 1994, J. Korean Astron. Soc., 27, 81
Reach, W. T., & Rho, J. 1996, A&A, 315, L277
Reach, W. T., Rho, J., & Jarrett, T. H. 2005, ApJ, 618, 297
Rho, J., Jarrett, T. H., Cutri, R. M., & Reach, W. T. 2001, ApJ, 547, 885
Shikaze, Y., et al. 2007, Astropart. Phys., 28, 154
Strong, A. W., Moskalenko, I. V., & Reimer, O. 2004, ApJ, 613, 962
Torres, D. F., Marrero, A. Y. R., & de Cea Del Pozo, E. 2010, MNRAS, 408, 1257
Uchiyama, Y., Aharonian, F. A., Tanaka, T., Takahashi, T., & Maeda, Y. 2007, Nature, 449, 576